

THE UV-CONTINUUM PROPERTIES OF LY α -SELECTED GALAXIES AT $Z = 6.5$

LENNOX L. COWIE¹ ESTHER M. HU¹ ANTOINETTE SONGAILA¹

Institute for Astronomy, University of Hawaii, 2680 Woodlawn Drive, Honolulu, HI 96822

To be published in Astrophysical Journal Letters

ABSTRACT

We report the first space-based very deep near-infrared continuum observations of a uniform sample of $z = 6.5$ galaxies with $\log(L(\text{Ly}\alpha)) = 42.5 - 43 \text{ erg s}^{-1}$ selected from narrow-band line searches and with spectroscopically confirmed Ly α emission. The $1.4\mu\text{m}$ HST WFC3 observations are deep enough ($\text{AB}(1\sigma) = 28.75$) to measure individual continuum magnitudes at this redshift for all of the objects. We compare the results with continuum-selected samples at the same redshift and find that Ly α emission is present in 24% of all galaxies with $M_{\text{AB}}(1350\text{\AA}) < -20$ at $z = 6.5$. The error in this quantity is dominated by systematic uncertainties, which could be as large as multiplicative factors of three. The Ly α galaxies are extended but small (size $< 1 \text{ kpc}$), and have star formation rates of approximately $10 M_{\odot} \text{ yr}^{-1}$. We find a mean $L(\text{Ly}\alpha)/\nu L_{\nu}$ at 1400\AA of 0.08, with the seven objects showing a range from 0.026 to 0.26, implying that there is little sign of destruction of the Ly α line. All of the properties of the $z = 6.5$ sample appear to be very similar to those of Ly α emitters at lower redshifts.

Subject headings: cosmology: observations — early universe — galaxies: evolution — galaxies: formation — galaxies: high redshift

1. INTRODUCTION

At all redshifts from $z = 0$ to $z = 7$ a fraction of galaxies can be detected in the Lyman alpha line of hydrogen (e.g. Cowie and Hu 1998; Deharveng et al. 2008; Hu et al. 2010; Ouchi et al. 2010; Vanzella et al. 2010). The Ly α line is easily detected in narrow-band imaging or blind spectroscopic surveys, and Ly α emission-line searches have been widely used to find high redshift galaxies. In addition, for the highest redshift galaxies, this line is the only spectroscopic signature that can be used to confirm the redshift of a galaxy selected on the basis of color properties. However, Ly α is a difficult line to interpret. Because the line is resonantly scattered by neutral hydrogen, determining its escape path and therefore its dust destruction is an extremely complex problem both theoretically (e.g., Neufeld 1991; Finkelstein et al. 2007) and observationally (e.g., Kunth et al. 2003; Schaerer & Verhamme 2008, Östlin et al. 2009). It is therefore critical to determine the ultraviolet continuum properties of the Ly α emitting galaxies (LAEs) in order to understand how to interpret them in terms of physical quantities such as the star-formation rate and to relate them to UV-continuum selected samples at the same redshift (e.g., Bouwens et al. 2010).

Extending this measurement to the highest redshifts possible is of considerable interest because the LAEs may be used as probes of the structure of the intergalactic gas at $z > 6$ (e.g., Dijkstra & Wyithe 2010, Tilvi et al. 2010, Dayal et al. 2011, Laursen et al. 2011). Since Ly α photons resonantly scatter off of neutral hydrogen, the Ly α emission from galaxies scatters from the line of sight as it propagates through the intergalactic medium (e.g. Loeb & Rybicki 1999; Zheng et al. 2010) potentially

reducing the strength of the observed Ly α . Thus the frequency of Ly α emitters relative to the UV continuum-selected galaxy population is potentially a function of the degree of ionization of the intergalactic medium and could be used to probe the epoch of reionization of the universe, at redshift $z > 6$ (e.g. Stark et al. 2010, 2011).

Here we extend the measurement of the UV-continuum properties of the LAEs to $z = 6.5$, the highest redshift where substantial samples of these objects exist, using very deep near-infrared continuum observations of a uniform sample of $z = 6.5$ LAEs obtained with the WFC3 camera on HST. These are the first observations deep enough to measure individual continuum magnitudes at this redshift for all the objects in this population and we find that their UV-continuum properties and the fraction of Ly α emitters relative to UV-continuum selected samples are very similar to that seen at lower redshift. The observations show no indication that the onset of reionization is at $z = 6.5$.

2. OBSERVATIONS

We obtained $1.4 \mu\text{m}$ (rest frame 1850\AA) continuum detections for a sample of 7 Ly α emitters (LAEs) at $z = 6.5$ in a 600 arcmin^2 region centered on the massive $z = 0.3$ galaxy cluster Abell 370. The sample was drawn from Hu et al.'s (2010) Ly α spectroscopic atlas of 88 $z = 5.7$ and 30 $z = 6.5$ galaxies. The Hu et al. Ly α emitters were chosen based on their narrow-band excess and their broad-band colors in very deep images obtained with the Suprime camera on the Subaru 8m telescope. They were then spectroscopically confirmed using the DEIMOS spectrograph on the Keck 10m telescope. They form a sample of objects with Ly α rest frame equivalent widths above 20\AA and $\log(L(\text{Ly}\alpha)) = 42.5 - 43 \text{ erg s}^{-1}$ in the selected redshift interval. These objects have narrow Ly α emission lines (velocity widths $150 - 300 \text{ km s}^{-1}$) and, as we shall show below, while they are small, they

¹ Visiting Astronomer, W. M. Keck Observatory, which is jointly operated by the California Institute of Technology, the University of California, and the National Aeronautics and Space Administration

are marginally spatially extended in the present observations. We therefore assume that they are powered by star formation and not by an active galactic nucleus.

We used the WFC3 camera on *HST* with the F140W filter to obtain $1.4\mu\text{m}$ observations of all of the $z = 6.5$ objects in the A370 field of that survey. Each of the $z = 6.5$ galaxies was observed for 2 orbits using the F140W filter of the WFC3 camera on *HST* (Mackenty et al. 2010). A four point dither pattern was used and repeated 3 times, giving a total exposure time of 4235s for each field. We used the combined drizzled images together with the calibration produced by the *HST* pipeline, but then removed a further background determined from the median average of the fields. The measured FWHM for faint stars in the images is 0.22 arcseconds. As we shall discuss below, the galaxies are small so, given the high spatial resolution of the *HST* images, we used $0.8''$ diameter magnitudes and corrected these to approximate total magnitudes using an offset of 0.15 magnitudes computed from the enclosed energy curves of the instrument. We measured the noise in the images by measuring the fluxes in random blank sky positions and found a 1σ noise level of 28.75 for the corrected $0.8''$ diameter magnitudes.

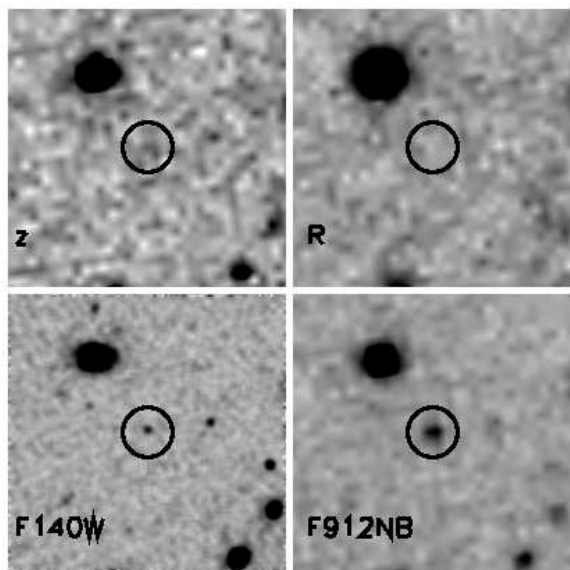


FIG. 1.— Comparison of the *HST* F140W observation for a typical object (HC023939-013451) with the ground based data from Hu et al. (2010). The lower left panel shows the F140W image, the lower right the 9120Å narrow band image, the upper left the z band image and the upper right the R band image. The circle marking the LAE is one arcsecond in radius.

All of the galaxies in the sample were detected; a typical example is shown in Figure 1. The faintness of the image, even in a very deep z band exposure such as that shown ($5\sigma \sim 25.4$ AB), illustrates the difficulty of making accurate continuum measurements from the ground. The observed continuum magnitudes and other quantities are listed in Table 1. The first detected $z = 6.5$ galaxy, HCM6A (Hu et al. 2002), is a member of the sample and since this galaxy lies in the strong-lensing region of A370, for this object we also give the values corrected for lensing amplification (quantities in paren-

theses in Table 1). All of the remaining galaxies lie far outside the strong lensing region and have negligible amplification.

For a comparison sample at $z = 5.7$ chosen in the same way and with comparably deep continuum magnitudes, we took Hu et al.’s sample of six $z = 5.7$ spectroscopically confirmed objects in the GOODS-N field, using published F850LP data obtained with the ACS on the *HST* (Giavalisco et al. 2004) to define our continuum magnitudes. The $z = 5.7$ magnitudes and errors are the auto mags from the catalog of Giavalisco et al. (2004); they also provide a good representation of the total magnitude. The rest-frame wavelength corresponding to the pivot wavelength of this filter is 1350\AA . While the F140W filter has no response at the $\text{Ly}\alpha$ line, the F850LP filter has 10% of peak response at 8140\AA ($\text{Ly}\alpha$ for $z = 5.7$). However, the emission-line contribution to the continuum fluxes is small ($< 20\%$) even for the highest equivalent width ($\text{EW} \approx 140\text{\AA}$) $z = 5.7$ galaxies. The properties of these objects are also listed in Table 1.

3. DISCUSSION

The LAE galaxies at both $z = 5.7$ and $z = 6.5$ are extremely compact (Figure 2). For each redshift sample we formed a stack by summing all the images, centering on the peak flux. For the $z = 6.5$ objects we excluded HCM6A, which is lensed, and HC023949–013121, which lies close to a bright galaxy. A comparison of the stacked continuum images of the two samples with the point spread function (PSF) determined from faint spectroscopically confirmed stars in the two fields, shows that images at both redshifts are extended: the deconvolved FWHM is $0.08''$ at $z = 5.7$ and $0.14''$ at $z = 6.5$, corresponding to sizes between 0.5 and 1 kpc. This is very similar to values measured for $\text{Ly}\alpha$ emitters (LAEs) at $z = 3.1$ (Bond et al. 2009, 2010), where both the UV continuum and the $\text{Ly}\alpha$ emission are seen to be sub-kpc. The sizes are smaller than those found by Taniguchi et al. (2009) at $z = 5.7$ but the Taniguchi measurements were made in a bandpass containing the $\text{Ly}\alpha$ line and it is possible that this could be increasing the measured size in their sample if the $\text{Ly}\alpha$ emission is more extended. The UV size measurements provide a reference for future measurements of the $\text{Ly}\alpha$ sizes, which will allow us to measure the extent of the $\text{Ly}\alpha$ scattering region in galaxies. Such measurements are difficult but may be possible with ground-based adaptive optics or space-based narrow-band measurements.

Figure 3 shows our primary result. For both samples we plot the ratio of $\text{Ly}\alpha$ luminosity to continuum luminosity redward of $\text{Ly}\alpha$ (or equivalently the rest-frame equivalent width of the $\text{Ly}\alpha$ line, to which the ratio is approximately proportional [Dijkstra & Westra 2010]) as a function of $\text{Ly}\alpha$ luminosity. Following Stark et al. (2010), we have assumed $f_\nu \sim \nu^0$ in computing the equivalent width. Adopting $f_\nu \sim \nu^{-0.8}$ as suggested in Taniguchi et al. (2009) would increase the equivalent widths by a multiplicative factor of 1.4 for the $z = 6.5$ systems and 1.1 for the $z = 5.7$ systems. However, we note that we focus less on the $\text{Ly}\alpha$ equivalent width than on the UV continuum luminosity, which is less sensitive to the assumed f_ν since the wavelength difference is smaller. Here too we assume $f_\nu \sim \nu^0$ in comparing the two redshifts. The $z = 5.7$

TABLE 1
GALAXIES IN THE SAMPLE

Name	RA(2000)	Dec(2000)	Redshift	$\log L(\text{Ly}\alpha)$ (erg s^{-1})	mag^a (AB)	Rest EW ^b (\AA)
HC023927-013523	39.863293	-1.589833	6.450	42.73	26.68 ± 0.16	64 ± 9
HC023939-013432	39.914417	-1.575667	6.549	42.76	26.03 ± 0.09	36 ± 3
HC023939-013451	39.914791	-1.581028	6.531	42.90	26.73 ± 0.17	97 ± 15
HC023949-013121	39.956711	-1.522667	6.564	42.99	$28.00^{+0.70}_{-0.42}$	357^{+329}_{-116}
HCM6A	39.978001	-1.559111	6.559	$43.41(42.75^c)$	$24.62(26.27^c) \pm 0.02$	44 ± 1
HC024001-014100	40.007500	-1.683388	6.545	42.72	$27.84^{+0.61}_{-0.39}$	175^{+134}_{-53}
HC024004-012252	40.017708	-1.381278	6.502	42.62	26.37 ± 0.12	37 ± 4
HC123607+620838	189.033004	62.14394	5.640	42.95	26.36 ± 0.12	86 ± 10
HC123558+621017	189.045471	62.17144	5.672	42.58	26.54 ± 0.18	42 ± 8
HC123613+620748	189.056106	62.12994	5.635	42.95	25.99 ± 0.15	60 ± 9
HC123651+621936	189.215240	62.32683	5.675	42.96	26.89 ± 0.24	140 ± 34
HC123652+622152	189.216751	62.36460	5.689	42.92	26.37 ± 0.22	79 ± 18
HC123717+621759	189.324677	62.29974	5.663	42.91	26.52 ± 0.15	89 ± 13

NOTE. — (a) Continuum magnitude in the AB system at $1.4 \mu\text{m}$ ($z = 6.5$) and $0.91 \mu\text{m}$ ($z = 5.7$). (b) Rest-frame equivalent width of the Ly α line calculated assuming a flat- f_ν spectrum for the continuum at wavelengths between Ly α and $\sim 1850 \text{\AA}$ (rest-frame; $z = 6.5$) or $\sim 1350 \text{\AA}$ (rest-frame; $z = 5.7$). (c) Values corrected for lensing amplification.

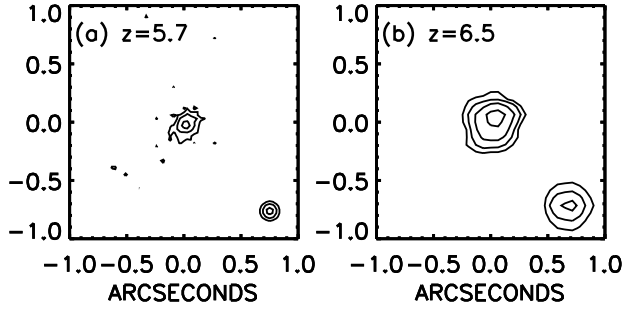


FIG. 2.— Stacked rest-frame near-UV images for (panel a) the $z = 5.7$ Ly α -selected galaxies and (panel b) the subset of isolated and unlensed $z = 6.5$ Ly α -selected galaxies. The point spread function measured from faint stars in the field is shown in the lower right corner. In both cases the images are resolved, though the effect is much more easily seen in the higher resolution ACS images of the $z = 5.7$ galaxies.

sample has identical median and mean values of 0.07 for the Ly α to UV continuum luminosity ratio, while the $z = 6.5$ sample has a median value of 0.05 and a mean value of 0.08. Both are very similar to that expected from a galaxy undergoing constant star formation. For a Salpeter initial mass function, the latter value is ≈ 0.065 almost irrespective of metallicity (Charlot & Fall 1993; Schaerer & Verhamme 2008). This value is shown as the solid black line in Figure 3. There is little sign of evolution with redshift, therefore, and, for this sample, little sign of destruction of the line relative to the continuum. The observed values catter above and below the average values by multiplicative values of roughly three. The high values may correspond to younger age, top-heavy IMF or particular escape geometry (e.g. Finkelstein et al. 2007).

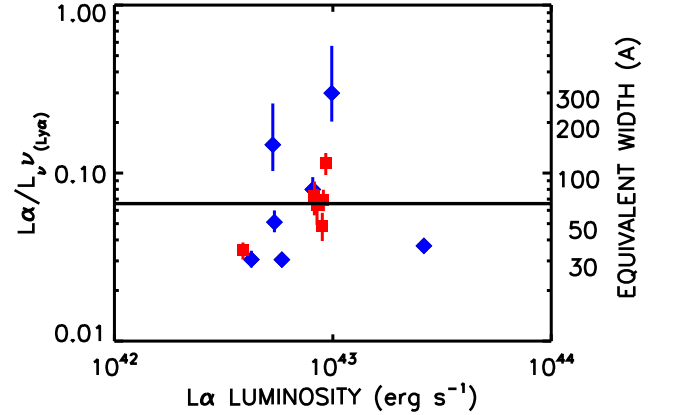


FIG. 3.— Fraction of light coming out in the Ly α line versus that coming out in UV continuum redward of Ly α . (The latter is calculated assuming a flat- f_ν continuum). This fraction is linearly related to the Ly α equivalent width which is given on the right hand vertical axis of the figure. Objects at $z = 6.5$ are shown with blue diamonds and objects at $z = 5.7$ with red squares. The error bars are $\pm 1 \sigma$.

The high value of the Ly α to UV continuum ratio is likely to be, at least in part, a selection effect: if there is a range in the amount of destruction of Ly α relative to the continuum, then the most luminous Ly α emitters will be those with the least destruction, which may then have near-standard ratios. In particular, objects without Ly α detections at the rest-frame EW limit of 20\AA should not be analyzed with this result, which holds only for objects in the LAE samples. However, the result does imply that many objects with little Ly α destruction do exist and that, for these luminous Ly α -selected objects, we can convert between Ly α and UV continuum luminosities. At first sight this may seem inconsistent with the blue asymmetric profiles seen in these Ly α emitters

(Hu et al. 2010). However, these profiles may be intrinsic to the galaxy and produced by scattering in outflows (Verhamme et al. 2006) rather than being a consequence of Ly α scattering in the surrounding intergalactic gas.

Our measured ratio of Ly α luminosity to UV continuum luminosity can be combined with the ‘conventional’ Kennicutt (1998) relation between the star formation rate and the UV luminosity to obtain $\log \text{SFR}(\text{M}_{\odot} \text{yr}^{-1}) = \log L(\text{Ly}\alpha) - 42.03$, where $L(\text{Ly}\alpha)$ is in erg s^{-1} and, again, the value is for a Salpeter initial mass function. The effects of metallicity may change this relation by as much as 0.2 dex (Schaerer & Verhamme 2008) and it is also dependent on the exact star formation history. However, it can be seen from the Ly α luminosities in Table 1 that typical star formation rates, with no extinction correction, are in the range of 5–10 $\text{M}_{\odot} \text{yr}^{-1}$, where we have used the relationship above in computing the SFRs. The UV continuum-selected galaxies without detected Ly α may have much more substantial Ly α destruction and for these the conversion rate from Ly α luminosity to SFR may be larger than the relation given above.

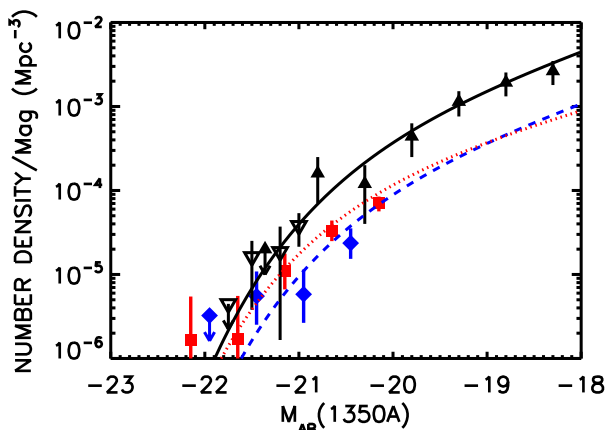


FIG. 4.— Ly α -selected 1350 \AA continuum luminosity functions at $z = 5.7$ (red squares) and $z = 6.5$ (blue diamonds) derived from the Hu et al. (2010) Ly α sample at these redshifts. Errors are $\pm 1\sigma$ and upper limits are 1σ and shown with a downward pointing arrow. The black filled triangles show the $z = 6.8$ luminosity function derived in Bouwens et al. (2010) and the open downward pointing triangles that of Ouchi et al. (2009) while the solid black curve shows the Bouwens et al. (2010) maximum likelihood Schechter-function fit to the combination of these two samples. The blue dashed curve is this fit renormalized by a factor of 0.24 in number density to match the Ly α -selected $z = 6.5$ continuum luminosity function. The red dotted curve is the $z = 5.9$ color-selected continuum luminosity function from Bouwens et al. (2010) renormalized by a factor of 0.18 in number density to match the $z = 5.7$ Ly α -selected continuum luminosity function.

We can also now test whether the Ly α emitters are comparable in continuum luminosity to samples obtained using continuum color-selection. From the full LAE sample of Hu et al. (2010) we constructed continuum luminosity functions of the Ly α -selected sample at both $z = 5.7$ and $z = 6.5$, using the accessible volumes computed for each object in Hu et al. We converted Ly α luminosity to a UV continuum luminosity at 1350 \AA (rest-

frame) using the constant star-formation value of 0.065 for the ratio of Ly α luminosity to UV continuum light redward of Ly α , and assuming the continua are roughly constant in f_{ν} from 1350 \AA to 1850 \AA . These luminosity functions are shown in Figure 4, where we compare them with continuum luminosity functions determined from color-selected samples (Ouchi et al. 2009; Bouwens et al. 2010). The Ly α -selected objects have high continuum luminosities (or equivalently star formation rates), comparable to the brightest continuum-selected objects at these redshifts. Our UV continuum luminosity function is lower by a factor of 5 than those derived by Shimasaku et al. (2006) and Kashikawa et al. (2006) whose results would imply that all UV continuum-selected objects at this redshift would also be LAEs. Both of these results may be due in part to the extreme difficulty of measuring accurate continuum magnitudes from ground-based data, particularly when the Ly α lines lie within the continuum bandpass. However, the difference is also due in part to the high Ly α luminosity functions calculated in these papers, which are about a factor of two above that of Hu et al. (2010). Hu et al. (2010) argue that the difference between their Ly α LF and the previous determinations is a consequence of using a fully spectroscopically confirmed sample which eliminates some of the photometrically selected objects but Kashikawa et al. (2011) argue against this interpretation. It is unclear therefore which is the better Ly α LF to choose, but we note that using the higher Kashikawa et al. (2011) Ly α LF would result in a very large fraction of UV continuum-selected galaxies having Ly α emission at near the case B ratio. This would be a rather surprising result, given that we expect at least some destruction owing to scattering in the IGM.

We can also use the luminosity functions to estimate the fraction of UV continuum sources that have strong Ly α emission. This fraction rises rapidly at low redshifts (from 5% at $z = 0$ to $\sim 20\%$ at $z = 2$; Cowie, Barger & Hu 2010) but above $z = 2$ it has been less clear whether it continues to increase or drops again (Stark et al. 2010, 2011; Zucca et al. 2009; Hayes et al. 2010). Above a UV continuum magnitude of -20.2 the Ly α sample comprises $24 \pm 6\%$ of the color-selected continuum sample at $z = 6.5$. For $z = 5.7$ the corresponding number is $18 \pm 2\%$ above -19.9 , where the errors are formal statistical errors. These fractions are very similar to those found at $z = 3$ by Shapley et al. (2003) for sources with similar rest-frame Ly α equivalent widths (above 20 \AA), which would suggest very little high-redshift evolution. It would represent a drop from the values at $z = 5.6 - 6.1$ found by Stark et al. (2011) who argue that nearly all continuum-selected objects at these redshifts are LAEs with rest-frame $\text{EW} > 20\text{\AA}$. However, we caution that the present numbers have substantial systematic uncertainties. The uncertainty in the UV to Ly α conversion ratio can result in significant changes: thus if the true conversion was 0.03 (0.13), the second lowest (second highest) value observed in the sample, the normalization would rise (fall) to approximately 0.6 (0.1). In addition, as we have discussed above, other measurements of the Ly α luminosity function at these redshifts (Kashikawa et al. 2006, 2011; Ouchi et al. 2008, 2010) have been a factor of two higher than Hu et al.’s and using these lu-

minosity functions would increase the LAE fraction by this amount. It is also possible that the UV continuum samples we are comparing with may still contain spurious objects, including red stars and lower redshift red galaxies, which would also increase the LAE fraction, and that there may be substantial uncertainties owing to cosmic variance in these continuum luminosity functions.

The present results show that LAEs at $z = 6.5$ have remarkably similar properties to those at lower redshifts. They are small, have moderately high star formation rates, and have substantially complete escape of the Ly α photons. Other properties such as the shape and widths of the Ly α lines also appear invariant (e.g. Ouchi et al. 2010, Hu et al. 2010). The results also show that the continuum luminosities are comparable to the brightest values seen in color-selected continuum samples, suggesting that even the strongest star-forming galaxies at these

redshifts may show Ly α in emission. We also find that the LAEs are a significant fraction of the UV-continuum selected objects at these redshifts, similar, within the systematic uncertainties, to values seen at lower redshifts. The observations show no sign that any effects associated with reionization are being seen at $z = 6.5$.

We gratefully acknowledge support from NSF grants AST-0709356 (L. L. C.), AST-0687850 (E. M. H.), and AST-0607871 (A. S.) and from Hubble Space Telescope HST-GO-11108.01-A (E. M. H.)

REFERENCES

- Bond, N. A., Gawiser, E., Gronwall, C., Ciardullo, R., Altmann, M., & Schawinski, K. 2009, *ApJ*, 705, 639.
- Bond, N. A., Feldmeier, J. J., Matković, A., Gronwall, C., Ciardullo, R., & Gawiser, E. 2010, *ApJ*, 716, L200.
- Bouwens, R., et al. 2010, arXiv:1006.4360.
- Cowie, L. L., Barger, A. J. & Hu, E. M. 2010, *ApJ*, 711, 928.
- Deharveng, J.-M., et al. 2008, *ApJ*, 680, 1074.
- Charlot, S., & Fall, S. M. 1993, *ApJ*, 415, 580.
- Dayal, P., Maselli, A., & Ferrara, A. 2011, *MNRAS*, 410, 830.
- Dijkstra, M. & Westra, E. 2010, *MNRAS*, 401, 2343.
- Dijkstra, M., & Wyithe, J. S. B. 2010, *MNRAS*, 408, 352.
- Finkelstein, S. L. et al. 2007, *ApJ*, 660, 1023.
- Gialaisco, M., et al. 2004, *ApJ*, 600, L93.
- Hayes, M., Schaerer, D., Östlin, G., Mas-Hesse, J. M., Atex, H., & Kunth, D. 2010, arXiv:1010.4796.
- Hu, E. M., Cowie, L. L., McMahon, R. G., Capak, P., Iwamuro, F., Kneib, J.-P., Maihara, T., & Motohara, K., 2002, *ApJ*, 568, L75 (erratum 576, L99).
- Hu, E. M., Cowie, L. L., Barger, A. J., Capak, P., Kakazu, Y., & Trouille, L. 2010, *ApJ*, 725, 394.
- Kashikawa, N., et al. 2006, *ApJ*, 648, 7.
- Kashikawa, N., et al. 2011, arXiv:1104.2330.
- Kennicutt, R. C., Jr. 1998, *ARAA*, 36, 189.
- Kunth, D. et al. 2003, *ApJ*, 597, 263.
- Laursen, P., Sommer-Larsen, J., & Razoumov, A. O. 2011, *ApJ*, 728, 52.
- Lehnert, M. D. et al. 2010, *Nature*, 467, 940.
- Loeb, A., & Rybicki, G. B. 1999, *AJ*, 524, 527.
- Mackenty, J. W., Kimble, R. A., O'Connell, R. W., & Townsend, J. A. 2010, *SPIE*, 7731, 27.
- Neufeld, D. A. 1991, *ApJ*, 370, L85.
- Östlin, G. et al. 2009, *AJ*, 138, 923.
- Ouchi, M., et al. 2008, *ApJS*, 176, 301.
- Ouchi, M., et al. 2009, *ApJ*, 706, 1136.
- Ouchi, M., et al. 2010, *ApJ*, in press.
- Schaerer, D., & Verhamme, A. 2008, *A&A*, 480, 369.
- Shapley, A. E., Steidel, C. C., Pettini, M., & Adelberger, K. L. 2003, *ApJ*, 588, 65.
- Shimizu, K. et al. 2006, *PASJ*, 58, 313.
- Stark, D. et al. 2010a, *MNRAS*, 408, 1628.
- Stark, D. P., Ellis, R. S. & Ouchi, M. 2011, *ApJ*, 2011, 728, L2.
- Taniguchi, Y. et al. 2009, *ApJ*, 701, 915.
- Tilvi, V. et al. 2010, *ApJ*, 721, 1853.
- Vanzella, E. et al. 2010, arXiv:1011.5500.
- Verhamme, A., Schaerer, D., & Maselli, A. 2006, *A&A*, 460, 397.
- Zheng, Z., Cen, R., Trac, H., & Miralda-Escudé, J. 2010, *ApJ*, 716, 574.
- Zucca, E., et al. 2009, *A&A*, 508, 1217.